Electromagnetically excited audible noise – evaluation and optimization of electrical machines by numerical simulation

C. Schlensok, B. Schmülling, M. van der Giet and K. Hameyer
Institute of Electrical Machines, Aachen, Germany

Abstract

Purpose – Disturbing vibrations and noise of electrical machines are gaining impact. The paper aims to focus on the necessity of estimating the electromagnetic, structure-dynamical, and acoustic behaviour of the machine during designing and before proto-typing.

Design/methodology/approach – An adequate tool is numerical simulation applying the finite-element method (FEM) and the boundary-element method (BEM) allowing for the structured analysis and evaluation of audible noise also caused by manufacturing tolerances.

Findings – The simulated results show good accordance to measurement results. The methods and simulation tools allow the analysis and evaluation of every type of energy converter with respect to its electromagnetic, structure-dynamical and acoustic behaviour.

Originality/value – The methods developed and proved can be applied to any electromagnetic device in general.

Keywords Simulation, Electric machines, Audibility, Noise control

Paper type Research paper

1. Introduction

The coupled physics of a complete acoustic simulation – starting from the electromagnetic force excitation, computing the mechanical deformation of the electromagnetic device and concluding in the estimation of the radiated audible noise – is a multi-physics problem. The central part of the computational chain is the electromagnetic field simulation of which the surface-force density-waves are derived. These excite the stator of the machine resulting in vibrations. The periodical oscillation of the machines surface is decoupled and radiated as disturbing audible noise.

For the numerical structure-dynamical and acoustic tool, a number of software programs have to be coupled, trimming the interfaces in a reasonable manner. This demands for a broad knowledge of the applied methods and their implementation. Therefore, an own tool box has been developed at the Institute of Electrical Machines (IEM) compatible to all types of electromagnetic devices such as transformers, rotating electrical machines (DC-, AC-machines, switched reluctance machines), actuators, and others (Arians *et al.*, 2006; van Riesen *et al.*, 2004; Zienkiewicz and Taylor, 1989; Kost, 1994; Bathe, 1986).

The structure of an entire acoustic multi-physics simulation-chain is shown in Figure 1 (Schlensok *et al.*, 2006). In a first step a FEM-model of the electromagnetic device

COMPEL: The International Journal for Computation and Mathematics in Electrical and Electronic Engineering
Vol. 26 No. 3, 2007
pp. 727-742

0332-1649
DOI 10.1108/03321640710751181

is simulated. A systematic, parameter-oriented model allows for a large number of geometry variations. Furthermore, various modes of operation can be considered. Hence, the effects of manufacturing tolerances can be taken into account as well as the designed geometry of the device (Schlensok and Henneberger, 2004). The electromagnetic model provides the normal component of the surface-force density on the elements used as excitation for the structure-dynamical model. In the mechanical model various materials and geometries can be considered to analyse the vibration. Here, the variants of the electromagnetic model are considered as parameters. In the last step the audible noise of the multitude of variants is estimated and analysed with an acoustic Boundary-Element (BEM) model (Brebbia, 1978; Brebbia, 1984; Brebbia *et al.*, 1984; Hartmann, 1989).

The acoustic simulation chain allows for the a-priori analysis of several machine variants at various modes of operation (e.g. operation on the grid or on a converter). An aimed systematic optimisation of the machine is performed based on this multi-physics problem. The resulting quantities are the sound pressure, the acoustic power of the sound pressure, the sound-particle velocity, and the sound intensity. In the following the three links of the simulation chain are discussed and examples show the efficiency of the applied tools.

2. Electromagnetic field computation

As example for the electromagnetic field problem, an electrical machine is studied. For the solving of the problem the FEM is applied. The FEM can be used for the simulation of 2D as well as 3D electromagnetic field problems. These can be static, time harmonic or transient. Therefore, the type of field problem has to be defined first. In the case of a long electrical machine the end effects can be neglected. If, furthermore, the flux paths are in the orthogonal plane to the rotor axis, a 2D FEM-model can be applied. For special 3D geometry effects such as skewing 2D models can be applied as well by interconnecting several 2D models (Boualem and Piriou, 1998; Dziwniel *et al.*, 2000; Dziwniel *et al.*, 1999; Piriou and Razek, 1990; Williamson *et al.*, 1990; Williamson *et al.*, 1995; Gyselinck *et al.*, 2001; Ho and Fu, 1997; de Oliveira *et al.*, 2004). In general, all the other cases require 3D models. The simulation of 2D FEM-models shows some significant advantages over 3D models:

Two-dimensional models are much smaller. Often the number of elements N_{el} is more than ten times lower as in the 3D model.

The computation time of electromagnetic model rises disproportionately with N_{el}. Therefore, 2D models result in least computational costs.

In general, the discretisation of the geometry is finer and hence the accuracy increases since there are more elements in the cross section of the geometry than in the case of a 3D model. Using the same discretisation (element size) in the 3D model results in a non-reasonable high N_{el}. Therefore, 2D FEM-models should be applied whenever possible.

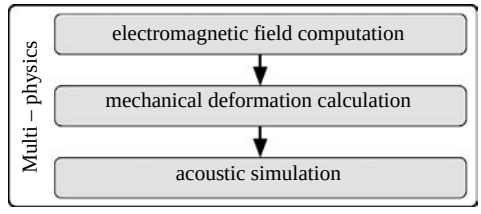

Figure 1.
Structure of the entire acoustic simulation-chain

In this paper an induction machine (IM) with squirrel-cage rotor and a switched reluctance machine (SRM) are studied. Both electrical machines are simulated electromagnetically applying appropriate 2D FEM-models. The process is exemplarily described for the IM in the following.

The electromagnetic FEM-model of the IM, shown in Figure 2 consists of the stator- and rotor laminations, the aluminium rotor bars, the copper winding of the stator, and the air gap. All other parts of the IM are not modelled since they have no significant impact on the electromagnetic field in the IM. The boundaries of the IM at the shaft and the outer circumference are assigned with a Dirichlet boundary condition (tangential magnetic field).

The electromagnetic simulation is performed in the time domain. A *quasi-static* model of the IM computed for a fixed number of time steps N applying a transient solver (Arians *et al.*, 2006; Albertz and Henneberger, 2000; De Gersem *et al.*, 2004). At each time step the rotor is rotated depending on the rotor speed n and the time-step Δt:

$$\Delta\alpha = \frac{180^\circ}{60^\circ}(n\Delta t). \tag{1}$$

After rotating and re-meshing the air gap an appropriate stator current is assigned to the model and the flux-density distribution of the previous time step is taken into consideration for the right-hand side of the equation system. Hereby, the transient relaxation factor θ weights the previous solution (Zienkiewicz and Taylor, 1989). At IEM electromagnetic simulations are usually performed using the Galerkin scheme by setting $\theta = 2/3$. By this, fast convergence is assured. Each of the models (one FEM-model per time step) represents a static electromagnetic field problem. From each of the field problems the magnetic vector potential results. Figure 3 shows the magnetic vector potential for one time step. The four magnetic poles of the machine can be easily recognised. The flux-density distribution is given by:

$$\vec{B} = \mathrm{rot}\,\vec{A} \tag{2}$$

with $\vec{A}$ being the magnetic vector potential.

The flux-density distribution in Figure 4 shows that the highest values of B are reached in the tooth tips. Furthermore, the mounting kerfs on the outer circumference

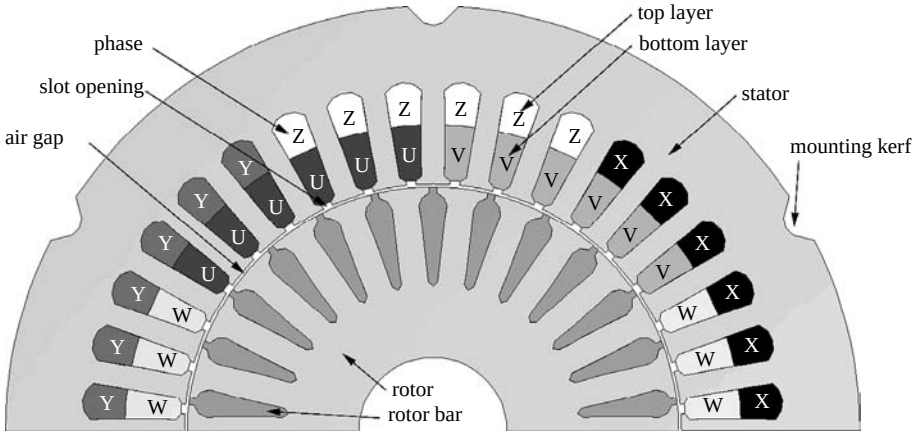

Figure 2.
Electromagnetic, 2D model of the IM

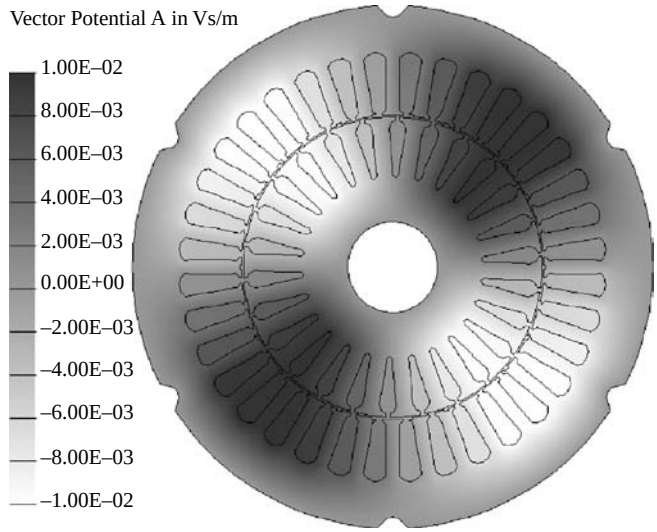

Figure 3.
Magnetic vector potential in the IM for one single time step

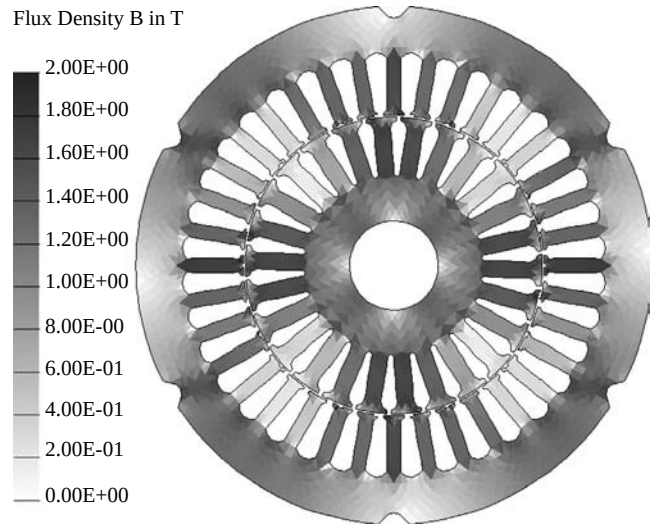

Figure 4.
Flux-density distribution in the IM for one single time step

of the IM have some impact on the flux paths, constricting the flux and increasing the flux density slightly. Since, the resulting values are below the saturation point of the iron lamination this has no significant effect on the motor's operational behaviour.

The number of simulation time steps N has to be chosen depending on the resolution of the spectrum of all required quantities. The preferred resolution of the spectrum of the surface-force density used as excitation for the structure-dynamical simulation has to be considered here. Both, the cut-off frequency f_{co} of the spectrum and the resolution Δf depend on Δt and N with Shannon's sampling theorem (Lüke, 1999):

$$\Delta f = \frac{1}{2\Delta t N} \tag{3}$$

$$f_{co} = \frac{1}{2\Delta t}. \tag{4}$$

From the flux-density distribution the torque T, the net force F, the surface-force density σ, and other quantities are derived. For the acoustic simulation chain T and F are not of interest and therefore not regarded here. σ is calculated for each time step on the stator teeth using the Maxwell – stress tensor – method (Ramesohl *et al.*, 1996). In addition to, σ, some specific electromagnetic devices such as transformers (Kubiak and Witczak, 2002) afford the consideration of magnetostriction (Delaere, 2002; Bauer and Henneberger, 1999). In regular rotating electrical machines σ predominates in general (Jordan, 1950; Timar, 1989; Witczak *et al.*, 1998; Belmans and Hameyer, 2002). Therefore, magnetostriction and Lorentz forces are neglected and only σ is taken into consideration further on.

Figure 5 shows the resulting force excitation of a 3D IM-model for one time step. The skewing of the rotor is reflected by the skewed force distribution on the teeth. The included zoom of one of the stator teeth shows, that at motor operation the highest magnitudes appear on the up-running edge of the teeth.

The surface-force density of the marked first element (Figure 5) of the tooth is transformed to the frequency domain and analysed. Figure 6 shows the resulting spectrum. The frequencies detected result from the fundamental and the harmonic air-gap field-components of the stator which interact with the fundamental and harmonic components of the rotor (Jordan, 1950; Timar, 1989). The harmonics depend

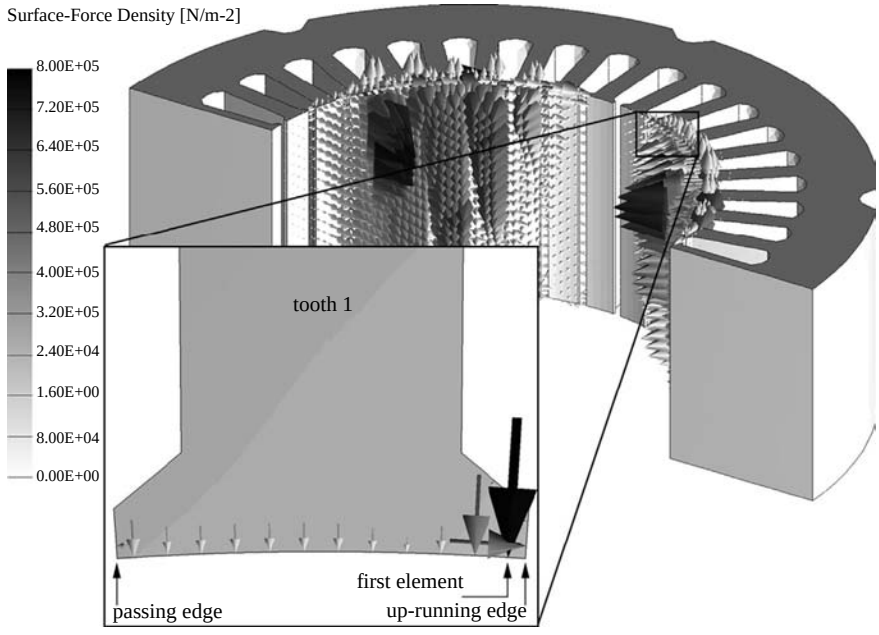

Figure 5.
Surface-force density-distribution on the stator teeth of the IM for one single time step

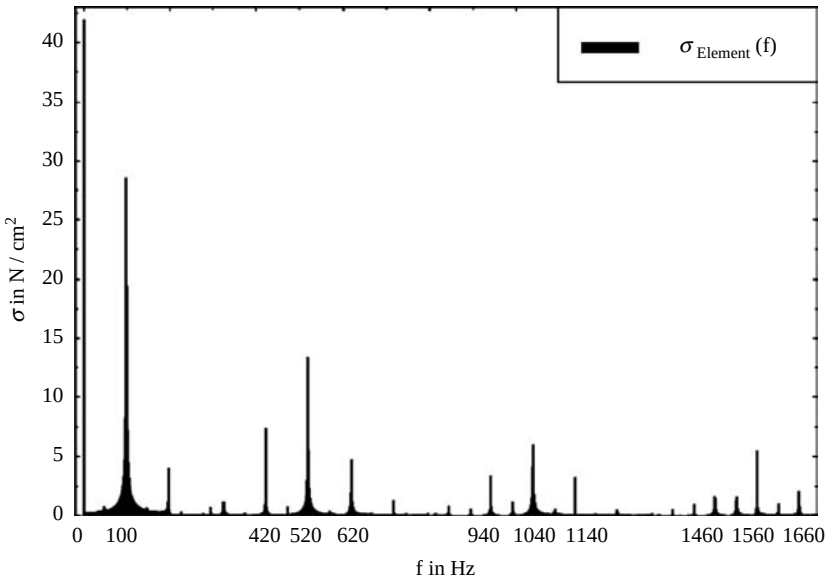

Figure 6.
Spectrum of the surface-force density of a single stator-tooth element

on the point of operation defined by the speed n, the slip s, and the stator frequency f_1 as well as the winding arrangements of rotor and stator described by the number of pole pairs p, the stator and rotor slot numbers N_S and N_R, and the number of phases m. Table I collects these parameters for the studied IM and the studied operation point.

From these parameters the significant harmonic frequencies are calculated (Jordan, 1950; Timar, 1989) listed in Table II. These frequencies are considered in the following structure-dynamical simulation of the IM described in the next section.

Table I.
Parameters and point of operation of studied IM

p	Pole-pair number	2
N_S	Number of stator slots	36
N_R	Number of rotor slots	26
m	Number of phases	3
n	Speed	1,200 rpm
f_1	Stator frequency	48.96 Hz
s	Slip	0.183

Table II.
Significant harmonic frequencies

$2\,f_1$	Double stator frequency	98 Hz
$N_R\,n$	1st rotor-slot harmonic	520 Hz
$2\,N_R\,n$	2nd rotor-slot harmonic	1,040 Hz
$N_S\,n$	1st stator-slot harmonic	720 Hz
$N_R\,n + 2\,f_1$	Modulated 1st rotor-slot harmonic	422 Hz
$N_R\,n - 2\,f_1$	Modulated 1st rotor-slot harmonic	618 Hz
$2\,N_R\,n + 2\,f_1$	Modulated 2nd rotor-slot harmonic	942 Hz
$2\,N_R\,n - 2\,f_1$	Modulated 2nd rotor-slot harmonic	1,138 Hz

3. Structure-dynamic calculation

After the electromagnetic simulation of an electrical machine, a structure-dynamical simulation is performed to determine the deformation or the oscillations. The surface-force density on the stator teeth, which is obtained from the electromagnetic simulation, is used as excitation. As in the electromagnetic case, the calculation of the periodic, mechanical deformation of electrical machines requires a numerical simulation. Owing to the large numbers and complexity of its components, it is not possible to find an exact analytical solution. The structure-dynamical simulation is performed by means of FEM (Arians *et al.*, 2006; van Riesen *et al.*, 2004; Zienkiewicz and Taylor, 1989; Bathe, 1986).

The deformation of the machine is represented by the displacement of the individual nodes of the mechanical FE-model (Schlensok *et al.*, 2006; Ramesohl *et al.*, 1996; Delaere, 2002). Strain and deformation are related by:

$$\boldsymbol{\varepsilon} = S \cdot \vec{u} \tag{5}$$

$$\text{with } S = \begin{bmatrix} \frac{\partial}{\partial x} & 0 & 0 & \frac{\partial}{\partial y} & 0 & \frac{\partial}{\partial z} \\ 0 & \frac{\partial}{\partial y} & 0 & \frac{\partial}{\partial x} & \frac{\partial}{\partial z} & 0 \\ 0 & 0 & \frac{\partial}{\partial z} & 0 & \frac{\partial}{\partial y} & \frac{\partial}{\partial x} \end{bmatrix}^{\mathrm{T}} \tag{6}$$

The correlation between the strain $\boldsymbol{\varepsilon}$ and the tension $\boldsymbol{\sigma}$ is given by Hooke's law. Neglecting initial strain and tension, this is expressed as:

$$\boldsymbol{\sigma} = H \cdot \boldsymbol{\varepsilon}, \tag{7}$$

where H is Hooke's matrix. Its entries are defined by Young's modulus E and Poisson's ratio μ of the corresponding material. For the case of isotropic and homogenous bodies, it has the following form:

$$H = \frac{E(1-\mu)}{(1+\mu)(1-2\mu)} \begin{bmatrix} 1 & \frac{\mu}{1-\mu} & \frac{\mu}{1-\mu} & 0 & 0 & 0 \\ \frac{\mu}{1-\mu} & 1 & \frac{\mu}{1-\mu} & 0 & 0 & 0 \\ \frac{\mu}{1-\mu} & \frac{\mu}{1-\mu} & 1 & 0 & 0 & 0 \\ 0 & 0 & 0 & \frac{1-2\mu}{2(1-\mu)} & 0 & 0 \\ 0 & 0 & 0 & 0 & \frac{1-2\mu}{2(1-\mu)} & 0 \\ 0 & 0 & 0 & 0 & 0 & \frac{1-2\mu}{2(1-\mu)} \end{bmatrix} \tag{8}$$

To decrease the computational effort to a reasonable measure, it is necessary to use equivalent materials in the simulation. For example, the laminated sheet stack of the stator is modelled as such an equivalent material with an anisotropic Hooke's matrix. The determination of its parameters relies on material identifying algorithms. One algorithm, which is used to obtain the material parameters of an electrical machine's stator, is the threshold-accepting method (Ramesohl and Henneberger, 1997).

The potential energy of a body due to strain reads:

$$\Pi_p = \int_{\Omega} \varepsilon^T \cdot H \cdot \varepsilon \mathrm{d}\Omega - \int_{\partial\Omega} \vec{u} \cdot \vec{\sigma} \cdot \varepsilon \mathrm{d}\partial\Omega, \tag{9}$$

where $\vec{\sigma}_s$ is the surface force density and Ω the volume of the body. The kinetic energy of an oscillating body reads:

$$T = \int_{\Omega} \frac{\rho}{2} \cdot \dot{\vec{u}}^2 \mathrm{d}\Omega, \tag{10}$$

with the mass density ρ of the body. The deformation-solver formulation is constructed using Hamilton's principle, i.e. minimising the Lagrange function:

$$L = T - \Pi_p, \quad \text{by} \tag{11}$$

$$0 = \frac{\mathrm{d}}{\mathrm{d}t}\left(\frac{\partial L}{\partial \dot{\vec{u}}}\right) - \left(\frac{\partial L}{\partial \vec{u}}\right) + \left(\frac{\partial F}{\partial \dot{\vec{u}}}\right), \tag{12}$$

where F represents a damping function. After discretising, the following oscillation equation is obtained:

$$K \cdot D + C \cdot \dot{D} + M \cdot \ddot{D} = F. \tag{13}$$

K is the global stiffness matrix, D is the vector of the node deformation, C is the damping matrix and F is the excitation force (Schlensok *et al.*, 2006). Owing to harmonic analysis, with:

$$\dot{D} = \frac{\mathrm{d}D}{\mathrm{d}t} = j\omega D \tag{14}$$

equation (12) becomes:

$$(K + j\omega C - \omega^2 M) \cdot D = F. \tag{15}$$

The complex surface force density F is transformed from the electromagnetic simulation to the mechanical model for each frequency to be analysed. Then, the structure-dynamical simulation is performed. This can be done either by solving equation (15) directly for each individual frequency separately, or by performing a modal analysis, i.e. finding the Eigen values and eigenvectors of the corresponding Eigen problem, together with a subsequent modal super-position. The appropriate approach for solving the equation (15) depends on the application. For the structure-dynamical simulation of electrical machines, solving equation (15) for each frequency individually has turned out to be advantageous in practice (Schlensok *et al.*, 2006).

The mechanical model (Figure 7) consists of all components of the electrical machine. The surrounding air is not included in the model, since for the expected small deformations of maximally a few micrometers, the influence of the air on the deformation of the solid body is negligible. Thus, the coupling between structure-dynamical and acoustic simulation can be considered a numerically weak coupling.

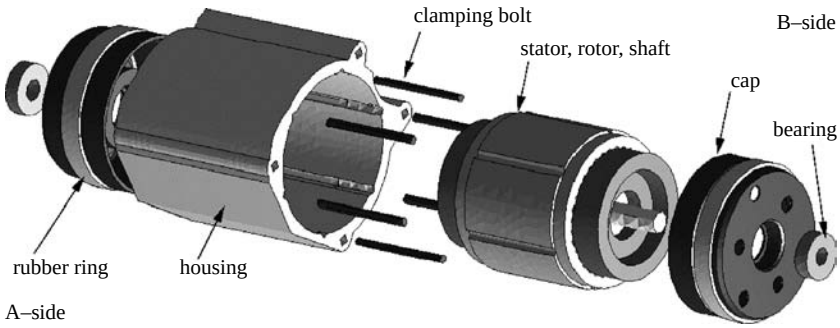

Figure 7.
Mechanical model (exploded view)

To achieve accurate values of the deformation of the entire machine structure, there are different requirements concerning the detailing of the individual parts. The rotor, for example, may be represented as a solid cylinder. The housing, however, has to be modelled with much more details. As in the electromagnetic case, extensive experience is required to set up a correct structure-dynamical model.

The deformation of an electrical machine can be evaluated as follows:

According to Jordan (1950), certain modes of oscillation ensue, which depend on stator frequency, speed, numbers of slots, the number of pole pairs and the winding arrangement. The modes of oscillation allow conclusions concerning the mechanical strength. In addition, it is possible to determine the expected single tones. Small mode numbers r are considered to be critical. With an increasing mode number, the mechanical structure becomes stiffer, and hence cannot be strongly deformed. A small deformation will enhance the acoustic behaviour. For example, mode number 1 is considered very critical, since it leads to large force excitations on to the bearings of the machine. Figures 8 and 9 show, for example, a deformation of the stator of an IM, with mode number $r = 6$. As studies have shown, manufacturing failures and asymmetries have a large impact on the deformation modes, and therefore on the acoustic behaviour of electrical machines.

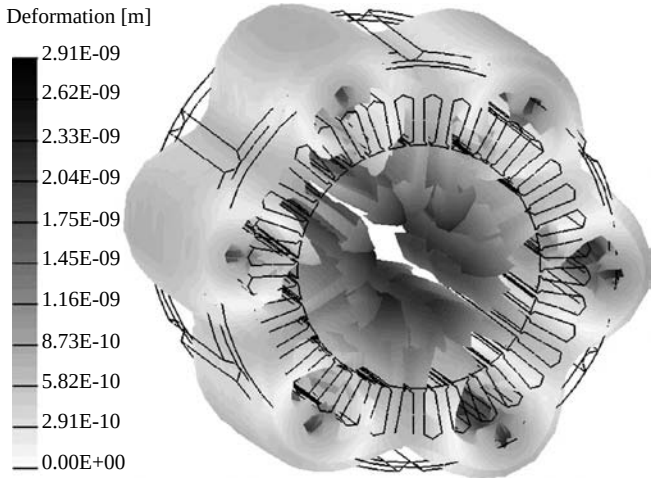

Figure 8.
Deformation of the stator at $f = 618$ Hz

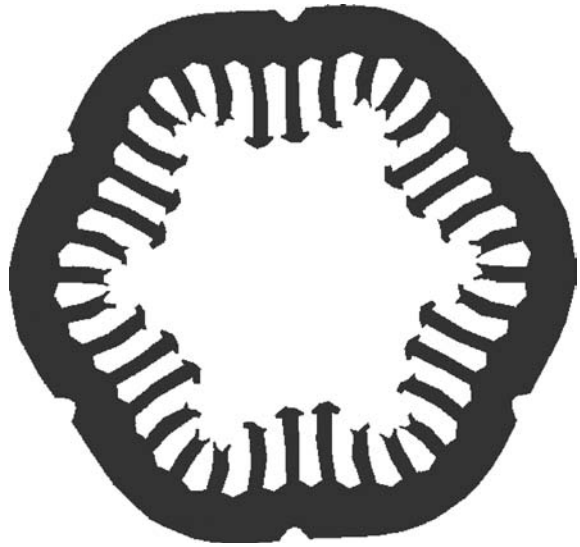

Figure 9.
Mode of deformation at $f = 618\,\text{Hz}$

Alternatively, the body sound-level can be determined at fixed locations, which may be identical to measuring positions. The advantage of this method is its comparability, its disadvantage, however, is its local scope. Therefore, the body sound-level does not provide conclusions about the behaviour of the complete structure.

Contrary to the body sound-level, the body-sound index represents an integral quantity for the complete body. Using this index, it is possible to globally compare the deformation for different excitations.

Depending on the technical question, the right evaluation criterion is to be chosen.

Owing to manufacturing tolerances, rotors of electrical machines are always mounted eccentrically. For the machine design, the bearing is considered ideal, and centric support is assumed. Therefore, it is necessary to estimate the effects of the eccentric support. Figure 10 shows the different rotational eccentricities, which are due to manufacturing tolerances. In the centric case, the centres of the rotor, of the stator and of the rotation are located at the same position. For the eccentric cases, either the centres of the rotation and of the rotor (dynamical eccentricity) differ, or the centres of the rotation and of the stator differ (static eccentricity). Both eccentricities can occur together as a combined static-dynamical eccentricity.

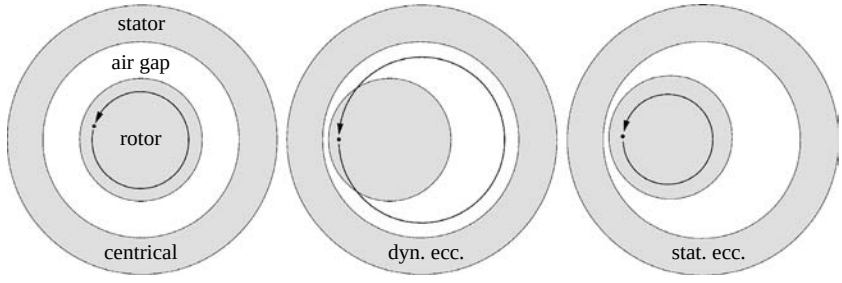

Figure 10.
Different rotational eccentricities of the IM

Figure 11 shows the results for selected frequencies of an induction motor at different eccentricities of the rotor compared to the centric machine. It shows that for an eccentric machine an increase in deformation has to be expected. The static eccentricity leads to the largest body sound-level, and has to be regarded very critical (Jordan, 1950). It further shows that it is not possible to conclude immediately the oscillation of an electrical machine from the excitation force density. For example, the largest deformation occurs for $N_S\ n = 720$ Hz ($N_S = 36$) despite very small force magnitudes (Figure 6).

4. Acoustic simulation

The acoustic noise radiated from electrical machines consists of three parts: the broad-band fan and ventilation noise (500-1,000 Hz) results in air turbulences generated by the rotating motor. Friction of the bearings of electrical machines is a further sound source, which generates single tones in the range larger than 3 kHz. Housing vibration excited by the electromagnetic field of electrical machines generates magnetic noise, which consists of single tones in the entire range of audibility. The presented calculation method only discusses the noise radiation generated by the electromagnetic deformation (vibration).

For the acoustic simulation, the mechanical deformation of the machine is converted to the velocity. In principle, calculation of acoustic fields is possible with the FEM. However, for calculation of air-borne noise this method is unfavourable, since the entire calculation area has to be discretised. An alternative is offered by the BEM (Schlensok *et al.*, 2006; Mai and Henneberger, 2000). Here, only the surface of the area is discretised. The basic principle of the BEM is the solution of the Helmholtz differential equation:

$$\Delta \underline{p} + k^2 \underline{p} = 0 \tag{16}$$

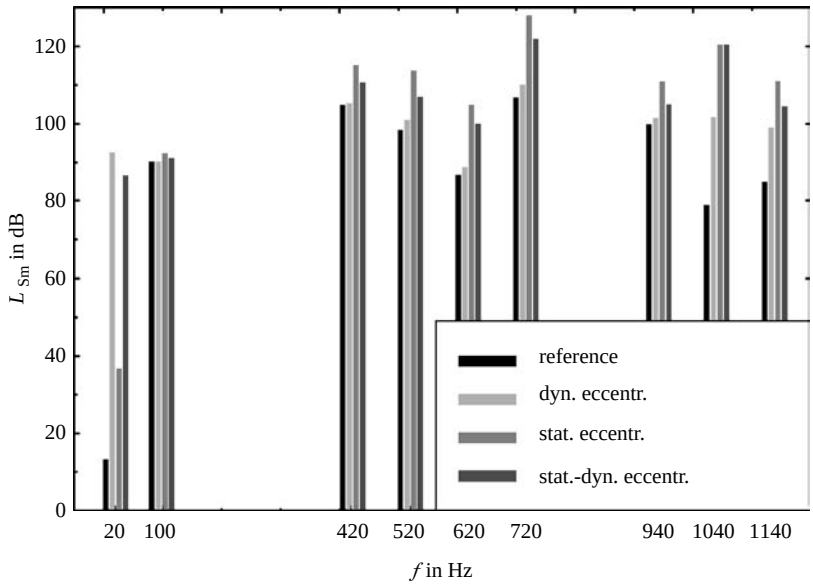

Figure 11.
Comparison of the body-sound index for eccentric models

with the sound pressure p and wave number $k = \omega/c$. Here, ω is the angular frequency and c the sound velocity. After further calculations the following equation system results:

$$H \cdot \underline{p} = G \cdot \underline{\vec{v}}. \tag{17}$$

H and G are system matrices (Schlensok *et al.*, 2006) and the velocity vector $\vec{v}$ serving as the excitation value. A numerical solution of equation (17) results in the sound pressure p. The used program was the procedure presented here. For the use of this method a third, acoustic model of the electrical machine is needed (additional to the electromagnetic and mechanical model). This model consists of the outer surface mesh only which represents the noise radiating area of the motor. The mechanical velocity is transferred to this acoustic mesh.

Since, the BEM is applied, there is no solution for the air volume surrounding the machine. Therefore, sound pressure and sound particle velocity are evaluated on predetermined points or surfaces (Figures 12 and 13). As further quantities acoustic power (Kollmann, 2000) and sound intensity of the machine are calculated. The results are available for discrete frequencies.

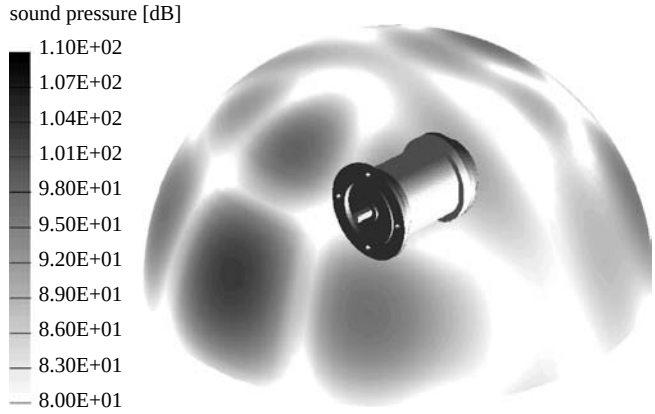

Figure 12.
Sound pressure distribution on the analysis sphere

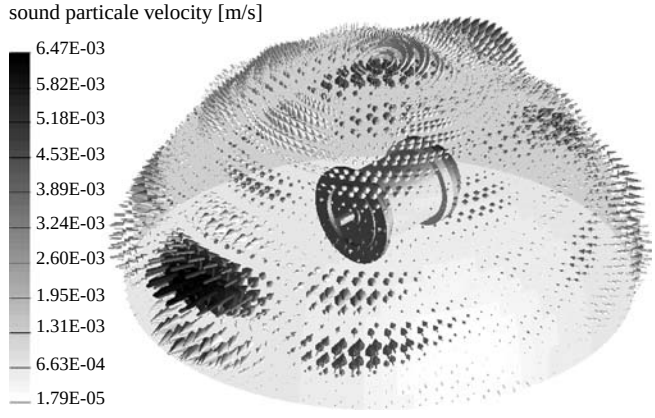

Figure 13.
Sound particle velocity field on the analysis sphere

Here, the evaluation of the acoustic simulation is presented for an SRM. Two current waveforms and two housing versions (aluminium and grey cast iron) are calculated for a selected operating condition. The simulated sound pressure and sound particle velocity are shown in Figure 11. The direction of noise radiation and acoustic power are determined by these quantities. At $f = 4{,}400$ Hz the SRM radiates the most acoustic noise in axial direction.

Figure 14 shows the results of both housing versions in the frequency range from 1,200 to 3,000 Hz. In the given example the noise radiation is also affected by the current waveform. Waveform 2 lowers the radiated noise.

The aluminium housing produces more acoustic noise than the cast iron housing. This is due to the higher material density of cast iron and the difference of the Young's modulus. The results agree good to sound measurements.

5. Conclusions

Numerical simulations allow for the consideration of the structure-dynamical and acoustic behaviour of an electrical machine a-priori during the phase of design. The proceeding of the numerical simulation is explained based on the considered machines (IM and SRM).

On the one hand, the simulated results show good accordance to measurement results, on the other hand the high optimisation potential concerning vibrations and noise of the analysed machines is presented. The presented methods and simulation tools allow the analysis and evaluation of every type of energy converter with respect to its electromagnetic, structure-dynamical and acoustic behaviour. By means of measurement devices it is also possible to verify the simulation results.

The analysis also provides the possibility of detecting manufacturing faults in electrical machines. Therefore, the numerical acoustic simulation is an essential tool for the design, validation and optimisation of electrical machines.

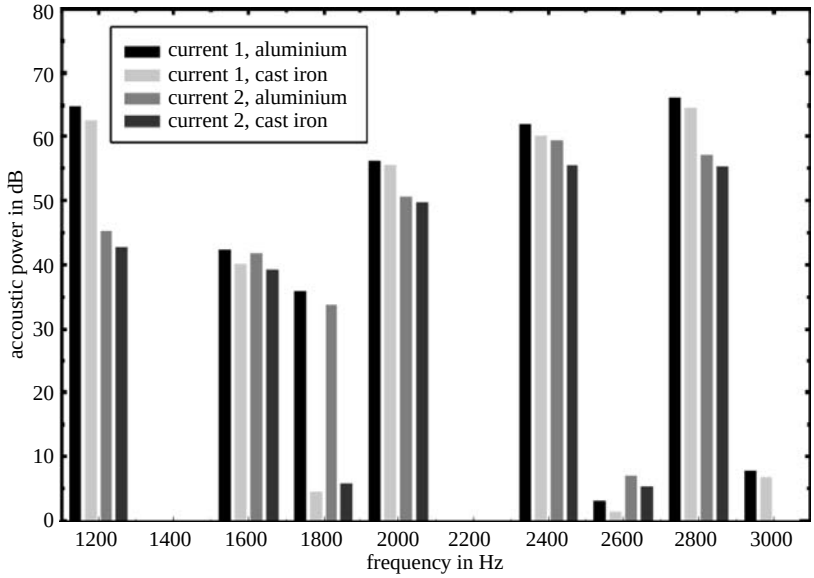

Figure 14.
Acoustic power for the studied operational condition of the SRM

References

Albertz, D. and Henneberger, G. (2000), "On the use of the new edge based A-A, T formulation for the calculation of time-harmonic, stationary and transient eddy current field problems", *IEEE Transactions on Magnetics*, Vol. 36 No. 4, pp. 818-22.

Arians, G., Bauer, T., Kaehler, C., Mai, W., Monzel, C., van Riesen, D. and Schlensok, C. (2006), "Innovative modern object-oriented solver environment – iMOOSE", available at: www.imoose.de.

Bathe, K-J. (1986), *Finite Elemente Methoden*, Springer-Verlag, Berlin.

Bauer, T. and Henneberger, G. (1999), "Three-dimensional calculation and optimization of the acoustic field of an induction furnace caused by electromagnetic forces", *IEEE Transactions on Magnetics*, Vol. 35 No. 3, pp. 1598-601.

Belmans, R. and Hameyer, K. (2002), "Impact of inverter supply and numerical calculation techniques in audible noise problems", paper presented at 1st International Seminar on Vibrations and Acoustic Noise of Electric Machinery, VANEM, Bethune, pp. 9-23.

Boualem, B. and Piriou, F. (1998), "Numerical models for rotor cage induction machines using finite element method", *IEEE Transactions on Magnetics*, Vol. 34 No. 5, pp. 3202-5.

Brebbia, C. (1978), *The Boundary Element Method for Engineers*, Pentech Press, London.

Brebbia, C. (Ed.) (1984), *Topics in Boundary Element Research*, Springer-Verlag, Berlin.

Brebbia, C., Telles, J. and Wrobel, L. (1984), *Boundary Element Techniques*, Springer-Verlag, Berlin.

De Gersem, H., Gyselinck, J.J.C., Dular, P., Hameyer, K. and Weiland, T. (2004), "Comparison of sliding-surface and moving-band techniques in frequency-domain finite-element models of rotating machines", *COMPEL*, Vol. 23 No. 3, pp. 1007-14.

de Oliveira, A.M., Antunes, P., Kuo-Peng, P., Sadowski, N. and Dular, P. (2004), "Electrical machine analysis considering field – circuit – movement and skewing effects", *COMPEL*, Vol. 23 No. 3, pp. 1080-91.

Delaere, K. (2002), "Computational and experimental analysis of electric machine vibrations caused by magnetic forces and magnetostriction", PhD-thesis, Katholieke University, Leuven.

Dziwniel, P., Piriou, F., Ducreux, J-P. and Thomas, P. (1999), "A time-stepped 2D-3D finite element method for induction motors with skewed slots modelling", *IEEE Transactions on Magnetics*, Vol. 35 No. 3, pp. 1262-5.

Dziwniel, P., Boualem, B., Piriou, F., Ducreux, J-P. and Thomas, P. (2000), ""Comparison between two approaches to model induction machines with skewed slots", *IEEE Transactions on Magnetics*, Vol. 36 No. 4, pp. 1453-7.

Gyselinck, J.J.C., Vandevelde, L. and Melkebeek, J.A.A. (2001), "Multi-slice FE modelling of electrical machines with skewed slots – the skew discretization error", *IEEE Transactions on Magnetics*, Vol. 37 No. 5, pp. 3233-7.

Hartmann, F. (1989), *Introduction to Boundary Elements Method*, Springer-Verlag, Berlin.

Ho, S.L. and Fu, W.N. (1997), "A comprehensive approach to the solution of direct-coupled multi slice model of skewed rotor induction motors using time-stepping eddy-current finite element method", *IEEE Transactions on Magnetics*, Vol. 33 No. 3, pp. 2265-73.

Jordan, H. (1950), *Geräuscharme Elektromotoren*, Verlag W. Giradet, Essen.

Kollmann, F.G. (2000), *Maschinenakustik*, Springer-Verlag, Berlin.

Kost, A. (1994), *Numerische Methoden in der Berechnung elektromagnetischer Felder*, Springer-Verlag, Berlin.

Kubiak, W. and Witczak, P. (2002), "Magnetostriction vibration of transformer core", paper presented at 3rd International Seminar on Vibrations and Acoustic Noise of Electric Machinery, VANEM, Lodz, pp. 71-5.

Lüke, H.D. (1999), *Signalübertragung*, Springer-Verlag, Berlin.

Mai, W. and Henneberger, G. (2000), "Object-oriented design of finite element calculations with respect to coupled problems", *IEEE Transactions on Magnetics*, Vol. 36 No. 4, pp. 1677-81.

Piriou, F. and Razek, A. (1990), "A model for coupled magnetic-electric circuits in electric machines with skewed slots", *IEEE Transactions on Magnetics*, Vol. 26 No. 2, pp. 1096-100.

Ramesohl, I. and Henneberger, G. (1997), "Automatic structural material identification of electrical machines using the threshold accepting procedure", paper presented at 11th Conference on the Computation of Electromagnetic Fields, Compumag, Rio de Janeiro.

Ramesohl, I., Henneberger, G., Küppers, S. and Hadrys, W. (1996), "Three dimensional calculation of magnetic forces and displacements of a claw-pole generator", *IEEE Transactions on Magnetics*, Vol. 32 No. 3, pp. 1685-8.

Schlensok, C. and Henneberger, G. (2004), "Comparison of static, dynamical and static-dynamical eccentricity in induction machines with squirrel cages using 2D-transient FEM", *COMPEL*, Vol. 23 No. 3, pp. 1070-9.

Schlensok, C., van Riesen, D., Küest, T. and Henneberger, G. (2006), "Acoustic simulation of an induction machine with squirrel-cage rotor", *COMPEL*, Vol. 25 No. 2, pp. 475-86.

Timar, P.L. (1989), *Noise and Vibration of Electrical Machines*, Elsevier, Oxford.

van Riesen, D., Monzel, C., Kaehler, C., Schlensok, C. and Henneberger, G. (2004), "iMOOSE – an open-source environment for finite-element calculations", *IEEE Transactions on Magnetics*, Vol. 40 No. 2, pp. 1390-3.

Williamson, S., Lim, L.H. and Smith, C. (1990), "Transient analysis of cage-induction motors using finite elements", *IEEE Transactions on Magnetics*, Vol. 26 No. 2, pp. 941-4.

Williamson, S., Flack, T.J. and Volschenk, A.F. (1995), "Representation of skew in time-stepped two-dimensional finite-element models of electrical machines", *IEEE Transactions on Magnetics*, Vol. 31 No. 5, pp. 1009-15.

Witczak, P., Kubiak, W., Mlotkowski, A. and Szulakowski, J. (1998), "Calculations of local magnetic forces in electric machinery", paper presented at 1st International Seminar on Vibrations and Acoustic Noise of Electric Machinery, VANEM, Bethune, pp. 57-61.

Zienkiewicz, O. and Taylor, T. (1989), *The Finite Element Method*,Vol. 1,2, McGraw-Hill, New York, NY.

About the authors

C. Schlensok received the MSc degree in electrical engineering in 2000 from the Faculty of Electrical Engineering and Information Technology at RWTH Aachen University. From 2001 to 2006 he has been researcher at the Institute of Electrical Machines (IEM) at RWTH Aachen University. In 2005, he obtained the PhD degree at the Faculty of Electrical Engineering and Information Technology at RWTH Aachen University with a thesis on numeric simulation and optimisation of induction machines. At the beginning of 2007 he moved to industry and is now a System Engineer at Bosch Rexroth AG in Lohr am Main. C. Schlensok is the corresponding author and can be contacted at: Christoph.Schlensok@iem.rwth-aachen.de

B. Schmülling received the MSc degree in electrical engineering in 2005 as Engineer from the Faculty of Electrical Engineering and Information Technology at the University of Dortmund. Since, 2005 he has worked as a researcher at the Institute of Electrical Machines (IEM) at RWTH Aachen University.

M. van der Giet received the MSc degree in electrical engineering in 2004 as Engineer from the Faculty of Electrical Engineering and Information Technology at RWTH Aachen University. Since, 2004 he has worked as a researcher at the Institute of Electrical Machines (IEM) at RWTH Aachen University.

K. Hameyer received the MSc degree in electrical engineering from the University of Hannover, Germany. He received the PhD degree from University of Technology Berlin, Germany. After his university studies he worked with the Robert Bosch GmbH in Stuttgart, Germany, as a Design Engineer for permanent magnet servo motors and board net components. In 1988 he became a member of the staff at the University of Technology, Berlin, Germany. Until February 2004 Professor Hameyer was a full Professor for Numerical Field Computations and Electrical Machines with the KU Leuven in Belgium. Currently, Professor Hameyer is the Director of the "Institute of Electrical Machines" and holder of the chair "Electromagnetic Energy Conversion" of the RWTH Aachen University in Germany. His research interests are numerical field computation, the design of electrical machines, in particular permanent magnet excited machines, induction machines and numerical optimisation strategies.